Title

A simple reverse genetics method to generate recombinant coronaviruses

Authors

Julien Mélade*, Géraldine Piorkowski, Franck Touret, Toscane Fourié, Jean-Sélim Driouich, Maxime Cochin, Hawa Sophia Bouzidi, Bruno Coutard, Antoine Nougairède & Xavier de Lamballerie.

* Corresponding author

julien.melade@univ-amu.fr

Affiliation

Unité des Virus Émergents (UVE: Aix-Marseille Univ-IRD 190-Inserm 1207), Marseille, France.

Abstract

Engineering recombinant viruses is capital for deciphering the biology of emerging viral pathogens such as the severe acute respiratory syndrome coronavirus 2 (SARS-CoV-2). However, the large size of coronaviruses genome makes reverse genetics methods challenging.

Here we describe a simple method based on “infectious subgenomic amplicons” (ISA) technology to generate recombinant infectious coronaviruses with no need for reconstructing a full genomic cDNA. The method was applied to the SARS-CoV-2 and the feline enteric coronavirus, and allowed to rescue wild-type viruses with biological characteristics closely similar to original strains. Mutations and fluorescent red reporter gene were rapidly incorporated into the SARS-CoV-2 genome allowing the generation of a genomic variant and a fluorescent reporter strains which were studied during *in vivo* experiments, serological diagnosis and antiviral assays.

The swiftness and simplicity of the ISA method has the potential to facilitate the advance of coronavirus reverse genetics studies and to explore biological properties of SARS-CoV-2 variants or accelerating the development of therapeutic measures.

Introduction

The order *Nidovirales* represents a large group of single-stranded positive-sense RNA viruses ((+) ssRNA) characterized by the size of their genomes, which are the largest among the RNA viruses. This order is subdivided into nine suborders including *Cornidovirineae* in which is found the *Coronaviridae* family. Coronaviruses (CoVs) have a wide range of hosts including humans, domestic and wild animals.

The severe acute respiratory syndrome coronavirus 2 (SARS-CoV-2; genus: *Betacoronavirus*) which emerged in 2019 in Wuhan, is responsible for COVID-19, a disease that has been associated in a proportion of patients with a severe pneumonia leading to respiratory distress and possibly to death[1,2]. SARS-CoV-2 has spread worldwide with more than 67 million people being infected by the end 2020. In the course of the pandemic, a European variant carrying an amino acid change in the spike protein (D614G) rapidly dispersed worldwide and became the most prevalent and dominant pandemic strain[3]. Later in 2020, others variants were detected in Denmark[4], South East England[5], Brazil[6] and South Africa[7]. The emergence of these variants raised questions concerning the possibility of viral escape from the immune response induced following either primary infection, vaccination or therapeutics applied as convalescent plasma[8]. The ongoing emergence of variants, their circulation and the genetic diversity observed in CoV populations highlight the need for convenient molecular tools to study viral evolution, replication, and pathogenesis and to enable the development of appropriate health control countermeasures.

Reverse genetics methods enable the engineering of wild-type or genetically modified CoVs and thus can contribute to deciphering biological properties of human or animal viruses[9,10]. In addition, they can be used to expedite antiviral screening for the selection and characterization of small antiviral molecules or therapeutic antibodies[11]. In the case of CoVs, rescue of infectious viruses can be obtained by the transfection of full-length cDNAs using vaccinia virus vectors or bacterial artificial chromosomes[10,12–14]. Alternatively, *in vitro* or in-yeast viral genome assembly followed by *in vitro* RNA production can lead to rescue viruses by transfection of full-length cDNAs in cells[15,16]. However, due to the complexity and large size of CoV genomes, the assembly and modification of full-length genomic cDNAs or RNAs remains laborious, technically difficult to reproduce and time-consuming (*e.g.* toxicity of clones, difficulty in constructing precise full-length 30 kb RNA transcripts *in vitro*).

The Infectious Subgenomic Amplicons (ISA) method is a simple and rapid bacterium-free method that has been developed in recent years for viruses with relatively short (+) ssRNA genomes, such as members of the *Flaviviridae*, *Togaviridae* and *Picornaviridae* families[17–21]. With the ISA method, wild-type and genetically modified infectious viruses can be recovered within days where conventional reverse genetics systems require additional cloning steps or *in vitro* manipulation of the RNA molecules. The ISA method is based on the simple transfection of overlapping subgenomic DNA fragments, encompassing the entire virus genome into permissive cells. DNA recombination and production of full-length viral genomic RNA, under transcription signals, are accomplished by the cellular machinery.

In the current study, we rescued the wild-type European variant of SARS-CoV-2 and the feline enteric coronavirus (FeCoV), a ubiquitous veterinary pathogen commonly circulating in felid populations and responsible for common enteritis [22] and the severe systemic disease, feline infectious peritonitis (FIP) [23]. We derived the original D614 coding sequence of the Wuhan SARS-CoV-2 by mutagenesis and added a mCherry fluorescent reporter gene. The characterization of each rescued strains performed *in vitro* and in a golden Syrian hamster model for SARS-CoV-2, and seroneutralization tests and antiviral assays were conducted using the mCherry fluorescent SARS-CoV-2 strain. Our results demonstrated the suitability of the strategy to study biological properties of viruses engineered using the ISA method.

Materials and Methods

Cells.

Baby Hamster Kidney 21 cells (BHK-21; ATCC CCL-10) were grown in Minimal Essential Medium (MEM; Life Technologies) with 5% heat-inactivated foetal calf serum (FCS), 1% L-glutamine (200mM; Life Technologies), 5% Tryptose Phosphate Broth (TPB; Life Technologies) and 1% Penicillin/Streptomycin (P/S; 5000 U/mL; 5 mg/mL). VeroE6 cells (ATCC CRL-1586) were grown in MEM supplemented with 5% FCS, 1% L-glutamine, 1% P/S and 1% non-essential amino acids (NEAA; Life Technologies). Feline embryonic fibroblast cells (FeA) were grown in Dulbecco's Modified Eagle Medium (DMEM; Life Technologies) with 10% FCS and 1% P/S. Feline pulmonary epithelial cells (AK-D; ATCC CCL-150) were grown in a mix of Ham's F12 (F12) and Leibovitz's (L-15) mediums (v/v) with 7% FCS and 1% PS. Cells were grown at 37 °C in an atmosphere containing 5% CO2.

Viral strains.

A clinical SARS-CoV-2 European strain was provided courtesy of Pr. Christian Drosten (Charité, Berlin) from the European Archive Collection (human isolate BetaCoV/Germany/BavPat1/2020 p.1; reference: 026V-03883). FeCoV was obtained from the American Type Culture Collection (ATCC reference: VR-2126). SARS-CoV-2 and FeCoV clinical samples were first passaged on VeroE6 and FeA respectively. An MOI of 0.001 and 0.01 were used to infect 12.5 cm2 culture flasks of confluent VeroE6 and FeA cells with the clinical SARS-CoV-2 and FeCoV respectively. Cells were washed twice (HBSS) 1 hour after the infection and 4mL of medium was added. Cell supernatant media were sampled at 48 hours post-infection, clarified by centrifugation, aliquoted and stored at −80°C. All experiments were conducted in a BSL3 laboratory.

Preparation of subgenomic cDNA fragments.

Based on full-length sequences, eight overlapping fragments were designed and supplied by the manufacturer (Genscript or Thermo Fisher Scientific). The first and last fragments were directly flanked at their 5’ and 3’extremities by the pCMV and the HDR/SV40pA respectively during *de novo* synthesis. To construct the D614 sequence and according to a Wuhan SARS-CoV-2 genome (Genbank accession number: NC045512), the Glycine (Gly) amino acid (GGT) located at position 614 of the spike protein in the fragment n°7 was replaced by an Aspartic acid (Asp) (GAT) and *de novo* synthesized (Thermo Fisher Scientific). From this construction, we inserted

a synthetic monomeric red fluorescent protein gene (mCherry) (Genbank accession number: AY678264) downstream of the regulatory sequence of the ORF3a (position 25392 – 26221) which was then *de novo* synthesized (Thermo Fisher Scientific). cDNAs were amplified from these *de novo* synthetic viral fragments as templates. A Super Fidelity PCR polymerase kit (Thermo Fisher Scientific) was used. Primer sequences and positions on genome are described in supplemental table 1**.** The final mixture contained 25µL of reaction mix, 2µL of DNA (1 ng/µL), 100 nM of each primer and 20µL nuclease-free water. RT-PCR and PCR reactions were performed on a Biometra TProfessional Standard Gradient thermocycler with the following conditions: 98 °C for 30s followed by 35 cycles of 98 °C for 10s, for X°C for 10s (Supplemental table 2), 72 °C for 30s/kb and 72 °C for 5 min and a preliminary step of 50 °C for 30 min for the RT-PCR. Amplicons were purified (Monarch® PCR & DNA Cleanup Kit; New England Biolabs) and the size of PCR products was verified by gel electrophoresis. All PCR products were sequenced to ensure that the genotypic integrity of each fragment was accurate before transfection.

Cell Transfection.

An equimolar mix (300 ng) of subgenomic cDNA fragments of SARS-CoV-2 and FeCoV was transfected into 96-wells of subconfluent BHK-21 cells and a coculture of BHK-21 + FeA cells respectively using Lipofectamine 3000 (Thermo Fischer Scientific). Lipofectamine and DNA were incubated for 45 minutes at room temperature and added to cells for 24 hours. These cell lines were selected after testing, in parallel, a panel of conditions (Supplemental table 3). For SARS-CoV-2, a suspension of VeroE6 cells was added 24 hours after transfection and then incubated for 5 days at 37°C in 5% CO_2. For FeCoV, fresh medium was added 24 hours after transfection and then incubated for 5 days at 37°C in 5% CO_2. Cell supernatant media were harvested and serially passaged 2 times to ensure the complete disappearance of the DNA used during transfection. Passages were performed by inoculating clarified supernatant media onto subconfluent VeroE6 and AK-D cells for SARS-CoV-2 and FeCoV respectively: after 1 h of incubation, cells were washed twice using Hanks' Balanced Salt solution (HBSS; Gibco), fresh medium was added, and plates were incubated for 2 days. After the last passage, cell supernatant media were harvested, clarified by centrifugation, aliquoted and stored at -80°C. These virus stocks were used to perform quantification of viral RNA, $TCID_{50}$ assay, sequencing and determination of kinetic reproduction.

Remdesivir antiviral activity on clinical and ISA SARS-CoV-2 strains.

The antiviral efficacy of Remdesivir on SARS-CoV-2 strains was assessed by determining the 50% and 90% effective concentrations (EC50 and EC90) as described in Touret *et al*., 2020 [25]. Briefly, one day prior to infection, 5×10^4 VeroE6 cells were seeded in 100µL assay medium (containing 2.5% FCS) in 96 well plates. The next day, eight two-fold serial dilutions of Remdesivir (from 20 to 0.15 µM, in triplicate (BLDPHARM, Shanghai, China) were added to the cells (25 µL/well, in assay medium). Four virus control wells were supplemented with 25µL of assay medium. After 15 min, 25µL of a calibrated virus mix diluted in medium was added to each well. Four cell control wells (i.e. with no virus) were supplemented with 25µL of assay medium. Plates were incubated for 2 days at 37 °C prior to quantification of the viral genome by real-time RT-PCR as described below. For fluorescence experiments, plates were analyzed on the same day immediately following supernatant medium collection for molecular biology, with the Incucyte ® S3 Live-Cell Analysis Systems (Sartorius) according to the manufacturer's instructions, with an acquisition time of 800 ms for the red channel. The percentage of fluorescent cells from an area was obtained using the Incucyte 2020B software (Sartorius). Dose response curves were generated using GraphPad Prism 7.00. EC50 and EC90 were estimated using logarithmic interpolation also with GraphPad Prism 7.00.

Human sera.

A total of 24 human sera (leftovers from volunteer donors who consented to non-therapeutic use of blood products) were tested for the presence of SARS-CoV-2 neutralizing antibodies (nAbs). All human sera were heat inactivated at 56°C for 30 min before anonymization and testing.

CPE and fluorescent based neutralization assay

To determine the level of SARS-CoV-2 nAbs, 110µL of twofold serial-diluted serum was pre-incubated with 110µL of 1,000 $TCID_{50}$/mL of SARS-CoV-2 strains in 5% FBS in DMEM for 60 min at 37°C. The virus–serum mixtures were then added into 96-wells plate of confluent monolayer Vero-E6 cells for 5 days at 37°C with 5% CO_2. The neutralization titer was defined as the highest dilution that inhibited the production of distinct CPE with the ISA D614 SARS-CoV-2 or fluorescence with the fluorescent mCherry D614 SARS-CoV-2. Samples with nAbs titers ≤10 were considered negative. In any of the duplicate testing wells was observed. The fluorescence signal was recorded using the Incucyte ® S3 Live-Cell Analysis Systems (Sartorius) with an acquisition time of 800 ms for the red channel.

In vivo experiments for SARS-CoV-2.

In vivo experiment in a hamster model were performed as previously described[26]. All experiments were approved by the local ethical committee (C2EA—14) and the French 'Ministère de l'Enseignement Supérieur, de la Recherche et de l'Innovation' (APAFIS#23975) and performed in accordance with the French national guidelines and the European legislation covering the use of animals for scientific purposes.

Animal handling

Female Syrian hamsters aged three-weeks-old were provided by Janvier Labs. Animals were maintained in ISOcage P - Bioexclusion System (Techniplast) with unlimited access to water/food and 14h/10h light/dark cycle. Every day, animals were weighed and monitored for the duration of the study to detect the appearance of any clinical signs of illness/suffering. Virus inoculation was performed under general anesthesia (isoflurane). Lungs and blood were collected after euthanasia (cervical dislocation) which was also realized under general anesthesia (isofluorane).

Hamster Infection.

Groups of 4 anesthetized animals (four-week-old) were intranasally infected with 50µL containing 10^3 $TCID_{50}$ of virus in 0.9% sodium chloride solution. The mock group was intranasally inoculated with 50µL of 0.9% sodium chloride solution.

Organ collection.

Lung and blood samples were collected immediately after the time of sacrifice. Left pulmonary lobes were first washed in 10mL of 0.9% sodium chloride solution and then transferred to a 2mL tube containing 1mL of 0.9% sodium chloride solution and 3mm glass beads. They were crushed using the Tissue Lyser machine (Retsch MM400) for 20 min at 30 cycles/s and then centrifuged 10min à 16,200g. Supernatant media were transferred to a 2mL tube, centrifuged 10 min at 16,200g and stored at −80°C. One milliliter of blood was harvested in a 2mL tube containing 100µL of 0.5M EDTA (ThermoFischer Scientific). Blood was centrifuged for 10 min at 16,200g and stored at −80°C.

RT-qPCR assays.

Viral RNA was isolated from 100µL of cell supernatant medium using a QIAamp Viral RNA kit and RNase-Free DNase Set on the automated QIAcube (Qiagen) facility, following the

manufacturer's instructions. Relative quantification of viral RNA was performed using the express One-Step SuperScript® RT-qPCR (Invitrogen). To isolate viral RNA from tissues, 100µL of organ clarified homogenates, spiked with 10µL of internal control (bacteriophage MS_2)[27], were transferred into an S-block containing the recommended volumes of VXL, proteinase K and RNA carrier. The RT-qPCR reaction mixture (for SARS-CoV-2 and MS2 viral genome detection) was processed using the GoTaq Probe 1-Step RT-qPCR kit (Promega) and contained 5µL of Master Mix 2X, 0.25µL of each primer (500 nM), 0.07µL of probe (75 nM), 0.2µL of GoScript RT mix, 0.4µL of H_2O and 3.8µL of extracted nucleic acids. Assays were performed using the QuantStudio 12K Flex Real-Time PCR machine **(**ThermoFisher Scientific) with the following conditions: 50°C for 15 min and 95°C for 2 min, followed by 45 cycles of 95°C for 3 s and 60°C for 30 s. Data collection occurred during the 60°C step. The amount of viral RNA was calculated from standard curves using synthetic RNA. The primers and probes used are described in supplemental table 4.

Tissue Culture Infectious Dose 50 ($TCID_{50}$) assay.

Subconfluent cultures of VeroE6 and AK-D cells in 96-well culture microplates were used for SARS-CoV-2 and FeCoV respectively $TCID_{50}$ determination. Cells were inoculated with 100 or 150µL per well of serial dilutions of each sample (four-fold or ten-fold dilutions when analyzing lung clarified homogenates or cell supernatant media respectively) and incubated for 3-6 days for each virus. Each row included 6 wells of the dilution and two negative controls. The presence of CPE in each well was used to determine $TCID_{50}$/mL. The determination of the $TCID_{50}$/mL for both viruses was performed using the Reed and Muench method [28].

Virus replication kinetics.

Infections at MOIs of 0.001 and 0.01 were performed using subconfluent VeroE6 or AK-D cells for SARS-CoV-2 and FeCoV, respectively. Cells were washed twice (HBSS) for 4 and 1 hours after infection with SARS-CoV-2 and FeCoV respectively and fresh medium was added. Cell supernatant media were sampled every 12 hours for up to 48 hours, clarified by centrifugation, aliquoted and stored at -80 °C. They were then analyzed using the RT-qPCR assay as described above. Each experiment was performed in triplicate.

Statistical analyses.

Exploratory analysis was performed using a two-way ANOVA with a Sidak's test correction. The correlation between CPE and fluorescent-based nAbs titers results was determined using a

linear regression model in the software Prism 7 (GraphPad). Pearson correlation coefficient (R^2) and *P* value are calculated using the default settings in the software Prism 7.00. Statistical analysis and graphical representation were performed using GraphPad Prism 7.00. *P* values ≤ 0.05 were considered statistically significant.

Results

General strategy for *de novo* production of CoVs

From each full-length genome sequence, 8 overlapping subgenomic fragments with an average size of 3,900 nucleotides were designed and *de novo* synthesized (Figure 1). During *de novo* synthesis, the human cytomegalovirus promoter (pCMV) was inserted upstream from the first fragment to initiate transcription. The sequence of the hepatitis delta virus ribozyme followed by the simian virus 40 polyadenylation signal (HDR/SV40pA) were added at the 3' end of the last fragment to enable transcription termination and RNA maturation (see previous studies[19,20]). The synthetic subgenomic viral fragments were used as templates for PCR amplification and transfected into permissive cells and passages 2 times on infected competent cells. Infectious viral particles were successfully obtained after two passages as confirmed by (i) observation of a cytopathic effect (CPE), (ii) measurement of the molecular viral load in cell supernatant medium using a real-time RT-qPCR assay, and (iii) measurement of the infectious viral load in cell supernatant medium using $TCID_{50}$ assays.

Generation of wild-type CoVs

First, we rescued wild-type infectious particles of the European SARS-CoV-2. At the second passage on VeroE6 cells, extensive CPE was observed from 2 days post-infection (dpi), as also observed with the clinical strain. The production of infectious particles was confirmed by the average molecular load (5.5±0.4 log_{10} RNA copies per mL) and infectious viral load (5.5±0.4 log_{10} $TCID_{50}$ per mL) detected at 2 dpi in the cell culture supernatant medium (Table). Replication kinetics were performed to compare the replicative fitness of the clinical and the rescued viruses. Clinical and ISA strains showed similar replication kinetics and no significant difference in molecular viral loads was observed post-infection (pi) (*N*=3; Two-way ANOVA*;* $p>0.05$) (Figure 2a).

We further evaluated the robustness of the ISA method to reconstruct a well-known and widespread felid coronavirus, FeCoV (Supplemental Figure S). After two passages of cell supernatant on FeA cells, extensive CPE was observed. The presence of rescued viral particles

was confirmed by the average molecular and infectious viral loads at 2 dpi in the cell culture supernatant medium (6.7±/-0.5 log_{10} RNA copies per mL and 5.8±/-0.6 log_{10} $TCID_{50}$ per mL, respectively) (Table). Comparative replication kinetics at an MOI of 0.01 did not show significant differences in virus yield (Figure 2b) from 12 hours until the endpoint (2 dpi) (*N*= 3; Two-way ANOVA*; p*>0.05) (Figure 2b).

Generation of the D614 SARS-CoV-2 strain

Early in the SARS-CoV-2 pandemic, several mutations were observed when comparing the original strain from Wuhan and the strain circulating in Europe. Among these mutations, the D614G on the spike protein sequence was suspected to contribute to changing the viral fitness[29,30]. To generate the spike protein D614 coding sequence in the ISA European strain, we substituted the Gly at position 614 of the spike protein sequence in the fragment n° 7 by an Asp and conducted the ISA method using this *de novo* synthesized modified DNA fragment (Figure 1). After 5 days post-transfection on BHK-21 and 2 dpi on VeroE6 cells, infectious particles were obtained and confirmed by CPE and molecular and infectious viral loads at 2 dpi in the cell culture supernatant medium (Table). Sequencing of the genomic fragment in which the modification was done indicated that the engineered D614 mutation in the spike protein was maintained after 2 passages in VeroE6 cells. Every 12 h pi, the molecular viral load in the supernatant medium of infected Vero E6 cells was recorded and analysed. Interestingly, significant differences were observed in early collections, particularly at 12h and 24h pi where molecular viral loads for the ISA D614 strain was 1.1±/-0.3 and 2.7±0.3 log_{10} RNA copies per mL respectively and 3.1±/-0.2 and 3.9±0.2 log_{10} RNA copies per mL respectively for the ISA European strain (Figure 2a) (*N*=3; Two-way ANOVA*; p*<0.05). At the endpoint, no significant difference was observed (48 h pi) between molecular viral loads for ISA D614 and European strains (4.6±/-0.2 and 4.7±0.1 log_{10} RNA copies per mL respectively) (*N*=3; Two-way ANOVA*; p*>0.05).

Generation of a fluorescent SARS-CoV-2

We next engineered a D614 SARS-CoV-2 strain containing a mCherry monomeric red fluorescent protein. The hypothetic dispensable 3a region[31] was removed and replaced by the mCherry protein sequence and *de novo* synthesized the modified DNA fragment for the ISA procedure (Figure 1). Following the ISA procedure, 5 days post-transfection on BHK-21 or 2 dpi on VeroE6 cells, infectious fluorescent mCherry D614 SARS-CoV-2 strain was recovered and similar cytopathic effect was observed at 48 pi. At an MOI of 0.05, red fluorescence was

readily detectable in the infected cells at 48 hours pi in comparison to the ISA D614 infected cells (Figure 3). The molecular and infectious viral loads detected at 2 dpi in Vero cell supernatant medium were indicated in Table. Sequencing of the genomic fragment in which the modification was done indicated that the engineered D614 mutation in the spike protein was maintained after 2 passages in VeroE6 cells. The mCherry D614 strain replicative fitness was assessed using the same conditions as previously described and compared with the ISA D614 SARS-CoV-2 strain. Replicative fitness was similar between fluorescent mCherry D614 and ISA D614 strains and no significant difference in molecular viral loads between each strain was recorded at any time pi (Figure 2).

Development and evaluation of neutralization and antiviral assays using the fluorescent mCherry SARS-CoV-2.

A seroneutralization assay was established by exploiting the fluorescence of the mCherry D614 SARS-CoV-2 for the endpoint readout and this was compared with a reference procedure[32] using the D614 strain, relying on the manual detection of CPE after image recording of the culture wells. Twenty-three human sera, collected during the COVID-19 pandemic, were tested for neutralization in the assay. Qualitatively, all the sera showing neutralization (18 out of 23) in the standard procedure performed equally well in the fluorescent procedure (Supplemental table 5) and all the negative sera in the CPE-based method were also negative in the fluorescence-based method. Titration of each serum with both methods indicated that seroneutralization titers were significantly correlated throughout the entire range of dilutions ($p < 0.0001$) with a correlation coefficient (R^2) of 0.8894 (Figure 4).

We next evaluated the mCherry D614 SARS-CoV-2 strain for an antiviral assay. Remdesivir was used as a reference compound known to inhibit the viral replication *in vitro* at the µM level[25,33]. The half-maximal effective concentration (EC50) was determined by monitoring the fluorescence in the presence of decreasing concentrations of Remdesivir (Figure 5a). The EC50 was compared to values obtained for both ISA D614 and mCherry D614 strains using a standard procedure relying on the quantification of the viral RNA yield[33]. The EC50 recorded for ISA D614 and mCherry D614 strains by RNA quantification were 1.4 µM (Figure 5b) and 0.6 µM (Figure 5b) respectively, suggesting that the insertion of the tag made the virus slightly more susceptible to the presence of the drug. The EC50 obtained by measuring the fluorescence of the mCherry D614 strain was in agreement with the EC50 obtained by the standard method (0.7 µM *vs* 0.6 µM), indicating that fluorescence reflects well the RNA viral load in the antiviral

assay (Figure 5b). Moreover, these values are also perfectly coherent with the microscopic observations were fluorescence and CPE inhibition were observed at 1.3 µM and 10 µM but not at 0.3 µM of Remdesivir concentration (Figure 5c).

Infection of Syrian hamsters with ISA viruses

A hamster model was used to study the clinical and virological properties of clinical and ISA-constructed SARS-CoV-2 strains. Groups of 4 animals were infected by intranasal inoculation of 10^3 $TCID_{50}$ of viruses. Clinical monitoring of animals infected by clinical and ISA SARS-CoV-2 showed a significant weight loss from 2 dpi when compared to animals inoculated with 0.9% sodium chloride solution (Two-way ANOVA; $p \leq 0.01$). From 0 to 4 dpi, infected animals expressed similar normalized weights (Two-way ANOVA; $p \geq 0.05$). However, from 5 to 7 dpi, animals infected by the clinical European strain or the ISA D614 strain expressed a greater weight loss than those infected with the ISA European SARS-CoV-2 (Two-way ANOVA; $p \leq 0.05$) (Figure 6a).

For each strain, viral infection and replication were confirmed as infectious virus was recovered from lungs and viral RNA was detected in lungs and plasma at 3 dpi. Analysis of virus replication in clarified lung homogenates revealed that mean infectious titers (measured using $TCID_{50}$ assay) were 6.6, 5.8 and 6.6 log_{10} $TCID_{50}$/g of lung, for animals infected with clinical European, ISA European and ISA D614 strains respectively. Infectious titers of virus recovered from hamsters infected by the ISA Wuhan strain were significantly lower than those rescued from hamsters infected with the clinical or the ISA European strains ($p \leq 0.01$) (Figure 6b). Mean viral RNA yields (measured using quantitative real time RT-PCR assay) were 9.2, 9 and 9.5 log_{10} copies/g of lung for animals infected with clinical European, ISA European and ISA D614 strains respectively. Viral RNA yields in lungs of hamsters infected by the ISA D614 strain were significantly higher than those of hamsters infected with the clinical European or the ISA European strains ($p \leq 0.05$) (Figure 6c). Analysis of virus replication in plasmas revealed no significant difference between the three strains ($p \geq 0.05$). Mean viral RNA yields (measured using quantitative real time RT-PCR assay) were 3.4, 5.0 and 4.2 log_{10} copies/mL respectively for animals infected with clinical European, ISA European and ISA D614 strains (Figure 6d).

Discussion

Reverse genetics methods are valuable modern tools to decipher biological properties of human and animal coronaviruses, mechanisms that underlie viral emergence and adaptation to the host, and to develop therapeutic strategies. Although coronaviruses have the largest genomes of known human RNA viral pathogens, several techniques were developed for the production of infectious clones before the emergence of the COVID-19 pandemic and they have been successfully adapted to the study of SARS-CoV-2 [15,16]. Nevertheless, these techniques rely on the cloning of a full-genome which is a relatively difficult and time-consuming process due to the large size of the coronavirus genome.

The ISA reverse genetics method overcomes this problem because no full length genomic cDNA cloning is involved in this procedure. In addition, the genome sequence of ISA-generated viruses can be identical to that of the targeted virus as no restriction sites or other genomic modifications are required. The method was originally developed for a variety of viruses with relatively short positive-stranded RNA genomes (*i.e.* <15,000 nucleotides) such as flaviviruses, alphaviruses or enteroviruses [18–21]. For these viruses, usually three overlapping subgenomic DNA fragments is sufficient to cover the full length genomic cDNA and to flank the 5' and 3' ends with a transcription start and a ribozyme/polyA signal, respectively. In the case of the much larger CoV genome, we found that by setting the number of subgenomic fragments to 8, the ISA method could be used to produce a wild-type and genetically modified CoV.

However, the recombination *in cellula* of such a high number of fragments had never been evaluated earlier. The objective therefore, was to assess whether or not we had reached the technical limitations of the method. Full length cDNA reconstitution implies two constraints: that cells generating infectious RNA should receive all fragments covering the entire virus genome, and that all fragments recombine together. An obvious consequence of this procedure is that the probability for an individual cell to receive all subgenomic fragments simultaneously upon transfection decreases when the number of fragments increases. Accordingly, in order to integrate the stochastic aspect of viral genesis in the ISA process, transfection/infection experiments can be conveniently performed in 96-well tissue culture plates with the product of 30 µg of mixed PCR fragments obtained from one single PCR reaction for each fragment.

Mutagenesis within the original sequence fragments can be accomplished using subgenomic sequences without jeopardizing subsequent genomic assembly. The resulting product is

immediately ready for the ISA procedure which can be exploited to decipher the mechanisms involved in viral evolution, transmission, pathogenesis and virus/host interactions [34–40].

We firstly designed and *de novo* synthesized a modified synthetic fragment to generate the G614D mutation in the Spike protein, as observed in the SARS-CoV-2 strain that was isolated in Wuhan, China. In our study, both European and D614 ISA strains displayed similar growth kinetics with similar viral RNA yields detected at the endpoint, suggesting that the D614 mutation does not *in fine* alter SARS-CoV-2 replicative fitness in VeroE6 cells, as it was previously observed in in another study[30].

The utilization of tagged viruses for neutralization or antiviral assays has been widely promoted as the presence of a reporter sequence enables direct monitoring of virus replication[41,42]. Viruses that incorporate a reporter tag can be valuable tools to characterize small molecules or nAbs that may inhibit virus replication, as the virus load can be monitored directly without the need for endpoint quantification of released genetic or infectious material. They can thus be used to improve and facilitate the process of seroneutralization assays or *in vitro* antiviral screening. In this study, an exogenous sequence such as the mCherry fluorescent reporter was stably inserted in the viral genome and enabled rescue of the tagged fluorescent virus. *In vitro* assays of the mCherry fluorescent strain on a panel of COVID-19 positive and negative human sera or against the antiviral drug, Remdesivir, demonstrated identical results with the wild-type strain. These procedures therefore open up new opportunities to implement robust and straight forward platforms for high throughput and low-cost sero-epidemiological studies. In line with the sero-neutralization assay, the mCherry virus can also be confidently used for antiviral screening and EC50 determination of antiviral compounds.

It is well established that golden Syrian hamsters provide a relevant animal model with which to study SARS-CoV-2 infection, pathogenesis and transmission[43]. In our study, both clinical and rescued SARS-CoV-2 strains replicated efficiently in infected hamsters and induced significant clinical symptoms. Interestingly, a lower weight loss associated with a lower infectious viral titer was observed with the ISA European SARS-CoV-2 infected group of animals in comparison with the clinical European strain. Similar results have been observed with Tick-borne [44,45] and it is recognized that clinical strains, often acting as quasispecies, are better adapted to their [46] environnement in comparison to clonal or quasi-clonal viruses. Here, it is assumed that the lower virulence of the ISA European SARS-CoV-2 *in vivo* could originate from a viral adaptation with generation of quasispecies and mutant spectrum.

In conclusion, we report an original and rapid reverse genetic procedure suitable for rescuing infectious coronaviruses under relatively simple operating conditions. The method was shown to be suitable for the *de novo* rescue of wild-type viruses and for the generation of mutated or engineered viruses. This unique and simplified reverse genetics method has the potential to accelerate significantly our comprehension of human and animal coronavirus pathogenesis, epidemiology, immunology and evolution. Moreover, it could also facilitate the further development of therapeutic and vaccine strategies.

Supplementary Data

Supplementary Data are provided online.

Acknowledgments

We thank Camille Placidi-Italia, Sarah Attoumani, Magali Gilles, Mariela Saba and Gregory Moureau for assistance in the experimental work. We kindly thanks Pr. Ernest Gould for reviewing this manuscript.

Funding

This work was supported by the European Virus Archive Global (EVA GLOBAL) funded by the European Union's Horizon 2020 research and innovation programme under grant agreement No 871029, the Fondation de France “call FLASH COVID-19”, project TAMAC and the Inserm through the REACTing (REsearch and ACTion targeting emerging infectious diseases) initiative.

Conflict of interest statement. None declared.

References

1. Zhou, P. *et al.* A pneumonia outbreak associated with a new coronavirus of probable bat origin. *Nature* **579**, 270–273 (2020).
2. Zhu, N. *et al.* A Novel Coronavirus from Patients with Pneumonia in China, 2019. *N. Engl. J. Med.* **382**, 727–733 (2020).
3. Korber, B. *et al. Spike mutation pipeline reveals the emergence of a more transmissible form of SARS-CoV-2*. http://biorxiv.org/lookup/doi/10.1101/2020.04.29.069054 (2020) doi:10.1101/2020.04.29.069054.
4. Kmec, L. Transmission of SARS-CoV-2 on mink farms between humans and mink and back to humans. 11 (2020).
5. Wise, J. Covid-19: New coronavirus variant is identified in UK. *BMJ* m4857 (2020) doi:10.1136/bmj.m4857.
6. Voloch, C. M. *et al. Genomic characterization of a novel SARS-CoV-2 lineage from Rio de Janeiro, Brazil*. http://medrxiv.org/lookup/doi/10.1101/2020.12.23.20248598 (2020) doi:10.1101/2020.12.23.20248598.
7. Tegally, H. *et al. Emergence and rapid spread of a new severe acute respiratory syndrome-related coronavirus 2 (SARS-CoV-2) lineage with multiple spike mutations in South Africa*. http://medrxiv.org/lookup/doi/10.1101/2020.12.21.20248640 (2020) doi:10.1101/2020.12.21.20248640.
8. Weisblum, Y. *et al.* Escape from neutralizing antibodies by SARS-CoV-2 spike protein variants. *eLife* **9**, e61312 (2020).
9. Stobart, C. & Moore, M. RNA Virus Reverse Genetics and Vaccine Design. *Viruses* **6**, 2531–2550 (2014).
10. Almazán, F. *et al.* Coronavirus reverse genetic systems: Infectious clones and replicons. *Virus Res.* **189**, 262–270 (2014).

11. Yang, C.-C. *et al.* A Novel Dengue Virus Inhibitor, BP13944, Discovered by High-Throughput Screening with Dengue Virus Replicon Cells Selects for Resistance in the Viral NS2B/NS3 Protease. *Antimicrob. Agents Chemother.* **58**, 110–119 (2014).
12. Thiel, V., Herold, J., Schelle, B. & Siddell, S. G. Infectious RNA transcribed in vitro from a cDNA copy of the human coronavirus genome cloned in vaccinia virus. 9 (2017).
13. Almazan, F. *et al.* Engineering the largest RNA virus genome as an infectious bacterial artificial chromosome. *Proc. Natl. Acad. Sci.* **97**, 5516–5521 (2000).
14. Yount, B., Curtis, K. M. & Baric, R. S. Strategy for Systematic Assembly of Large RNA and DNA Genomes: Transmissible Gastroenteritis Virus Model. *J. Virol.* **74**, 10600–10611 (2000).
15. Thi Nhu Thao, T. *et al.* Rapid reconstruction of SARS-CoV-2 using a synthetic genomics platform. *Nature* **582**, 561–565 (2020).
16. Xie, X. *et al.* An Infectious cDNA Clone of SARS-CoV-2. *Cell Host Microbe* **27**, 841-848.e3 (2020).
17. Atieh, T., Baronti, C., de Lamballerie, X. & Nougairède, A. Simple reverse genetics systems for Asian and African Zika viruses. *Sci. Rep.* **6**, 39384 (2016).
18. Atieh, T. *et al.* New reverse genetics and transfection methods to rescue arboviruses in mosquito cells. *Sci. Rep.* **7**, 13983 (2017).
19. Aubry, F. *et al.* Single-stranded positive-sense RNA viruses generated in days using infectious subgenomic amplicons. *J. Gen. Virol.* **95**, 2462–2467 (2014).
20. Aubry, F. *et al.* "ISA-Lation" of Single-Stranded Positive-Sense RNA Viruses from Non-Infectious Clinical/Animal Samples. *PLOS ONE* **10**, e0138703 (2015).
21. Touret, F. *et al.* Phylogenetically based establishment of a dengue virus panel, representing all available genotypes, as a tool in dengue drug discovery. *Antiviral Res.* **168**, 109–113 (2019).
22. Pedersen, N. C., Allen, C. E. & Lyons, L. A. Pathogenesis of feline enteric coronavirus infection. *J. Feline Med. Surg.* **10**, 529–541 (2008).
23. Pedersen, N. C. A review of feline infectious peritonitis virus infection: 1963–2008. *J. Feline Med. Surg.* **11**, 225–258 (2009).

24. Rothberg, J. M. *et al.* An integrated semiconductor device enabling non-optical genome sequencing. *Nature* **475**, 348–352 (2011).
25. Touret, F. *et al.* In vitro screening of a FDA approved chemical library reveals potential inhibitors of SARS-CoV-2 replication. *Sci. Rep.* **10**, 13093 (2020).
26. Driouich, J.-S. *et al. Favipiravir antiviral efficacy against SARS-CoV-2 in a hamster model*. http://biorxiv.org/lookup/doi/10.1101/2020.07.07.191775 (2020) doi:10.1101/2020.07.07.191775.
27. Ninove, L. *et al.* RNA and DNA Bacteriophages as Molecular Diagnosis Controls in Clinical Virology: A Comprehensive Study of More than 45,000 Routine PCR Tests. *PLoS ONE* **6**, e16142 (2011).
28. Reed, L. J. & Muench, H. A simple method of estimating fifty per cent endpoints. Am J Epidemiol. 27, 493–497 (1938).
29. Hou, Y. J. *et al.* SARS-CoV-2 D614G variant exhibits efficient replication ex vivo and transmission in vivo. *Science* eabe8499 (2020) doi:10.1126/science.abe8499.
30. Plante, J. A. *et al.* Spike mutation D614G alters SARS-CoV-2 fitness. *Nature* (2020) doi:10.1038/s41586-020-2895-3.
31. Yount, B. *et al.* Severe Acute Respiratory Syndrome Coronavirus Group-Specific Open Reading Frames Encode Nonessential Functions for Replication in Cell Cultures and Mice. *J. Virol.* **79**, 14909–14922 (2005).
32. Gallian, P. *et al.* Lower prevalence of antibodies neutralizing SARS-CoV-2 in group O French blood donors. *Antiviral Res.* **181**, 104880 (2020).
33. Wang, M. *et al.* Remdesivir and chloroquine effectively inhibit the recently emerged novel coronavirus (2019-nCoV) in vitro. *Cell Res.* **30**, 269–271 (2020).
34. Coutard, B. *et al.* The spike glycoprotein of the new coronavirus 2019-nCoV contains a furin-like cleavage site absent in CoV of the same clade. *Antiviral Res.* **176**, 104742 (2020).

35. Hoffmann, M., Kleine-Weber, H. & Pöhlmann, S. A Multibasic Cleavage Site in the Spike Protein of SARS-CoV-2 Is Essential for Infection of Human Lung Cells. *Mol. Cell* **78**, 779-784.e5 (2020).
36. Eckerle, L. D. *et al.* Infidelity of SARS-CoV Nsp14-Exonuclease Mutant Virus Replication Is Revealed by Complete Genome Sequencing. *PLoS Pathog.* **6**, e1000896 (2010).
37. Korber, B. *et al. Spike mutation pipeline reveals the emergence of a more transmissible form of SARS-CoV-2*. http://biorxiv.org/lookup/doi/10.1101/2020.04.29.069054 (2020) doi:10.1101/2020.04.29.069054.
38. Menachery, V. D. *et al.* Combination Attenuation Offers Strategy for Live Attenuated Coronavirus Vaccines. *J. Virol.* **92**, 15 (2018).
39. Muth, D. *et al.* Attenuation of replication by a 29 nucleotide deletion in SARS-coronavirus acquired during the early stages of human-to-human transmission. *Sci. Rep.* **8**, (2018).
40. Wang, J.-M., Wang, L.-F. & Shi, Z.-L. Construction of a non-infectious SARS coronavirus replicon for application in drug screening and analysis of viral protein function. *Biochem. Biophys. Res. Commun.* **374**, 138–142 (2008).
41. Xie, X. *et al.* A nanoluciferase SARS-CoV-2 for rapid neutralization testing and screening of anti-infective drugs for COVID-19. *Nat. Commun.* **11**, 5214 (2020).
42. Hou, Y. J. *et al.* SARS-CoV-2 Reverse Genetics Reveals a Variable Infection Gradient in the Respiratory Tract. *Cell* **182**, 429-446.e14 (2020).
43. Sia, S. F. *et al.* Pathogenesis and transmission of SARS-CoV-2 in golden hamsters. *Nature* **583**, 834–838 (2020).
44. de Fabritus, L., Nougair, A. & de Lamballerie, X. Utilisation of ISA Reverse Genetics and Large-Scale Random Codon Re-Encoding to Produce Attenuated Strains of Tick-Borne Encephalitis Virus within Days. *PLOS ONE* 11 (2016).
45. de Fabritus, L., Nougairède, A., Aubry, F., Gould, E. A. & de Lamballerie, X. Attenuation of Tick-Borne Encephalitis Virus Using Large-Scale Random Codon Re-encoding. *PLOS Pathog.* **11**, e1004738 (2015).

46. Domingo, E., Escarmís, C., Lázaro, E. & Manrubia, S. C. Quasispecies dynamics and RNA virus extinction. *Virus Res.* **107**, 129–139 (2005).

Table. Phenotypic characterization of rescued SARS-CoV-2 and FeCoV. For SARS-CoV-2 and FeCoV clinical and ISA strains, cell lines used for transfection and passage, presence or absence of cytopathic effect (CPE), quantification of the viral RNA by real-time RT-qPCR and infectious titers in cell supernatant media ($TCID_{50}$ assay) after 2 passages were summarized. Each experiment was performed in triplicate ($N = 3$). The infectious $TCID_{50}$ titer was expressed as log10 $TCID_{50}$/mL and the amount of RNA copies was expressed as log10 copies/mL.

		Cell line		CPE	Amount of viral RNA	Infectious titers
		Transfection	**Passage**			
SARS-CoV-2	Clinical European	-	VeroE6	Yes	7.1 +/- 0.2	7.6 +/- 0.1
	ISA European	BHK-21 + VeroE6	VeroE6	Yes	5.5 +/- 0.4	5.5 +/- 0.4
	ISA D614	BHK-21 + VeroE6	VeroE6	Yes	6.8 +/- 0.5	6.0 +/- 0.2
	mCherry ISA D614	BHK-21 + VeroE6	VeroE6	Yes	5.6 +/- 0.2	5.8 +/- 0.4
FeCoV	Clinical	-	FeA	Yes	7.6 +/- 0.2	7.2 +/- 0.2
	ISA	BHK-21 + FeA	FeA	Yes	6.7 +/- 0.5	5.8 +/- 0.6

Figure 1. **The ISA method to rescue SARS-CoV-2**. SARS-CoV-2 complete genome sequence was used to design eight overlapping subgenomic viral fragments covering the complete genome. Positions on the genome (in nucleotide) are indicated in bold red.

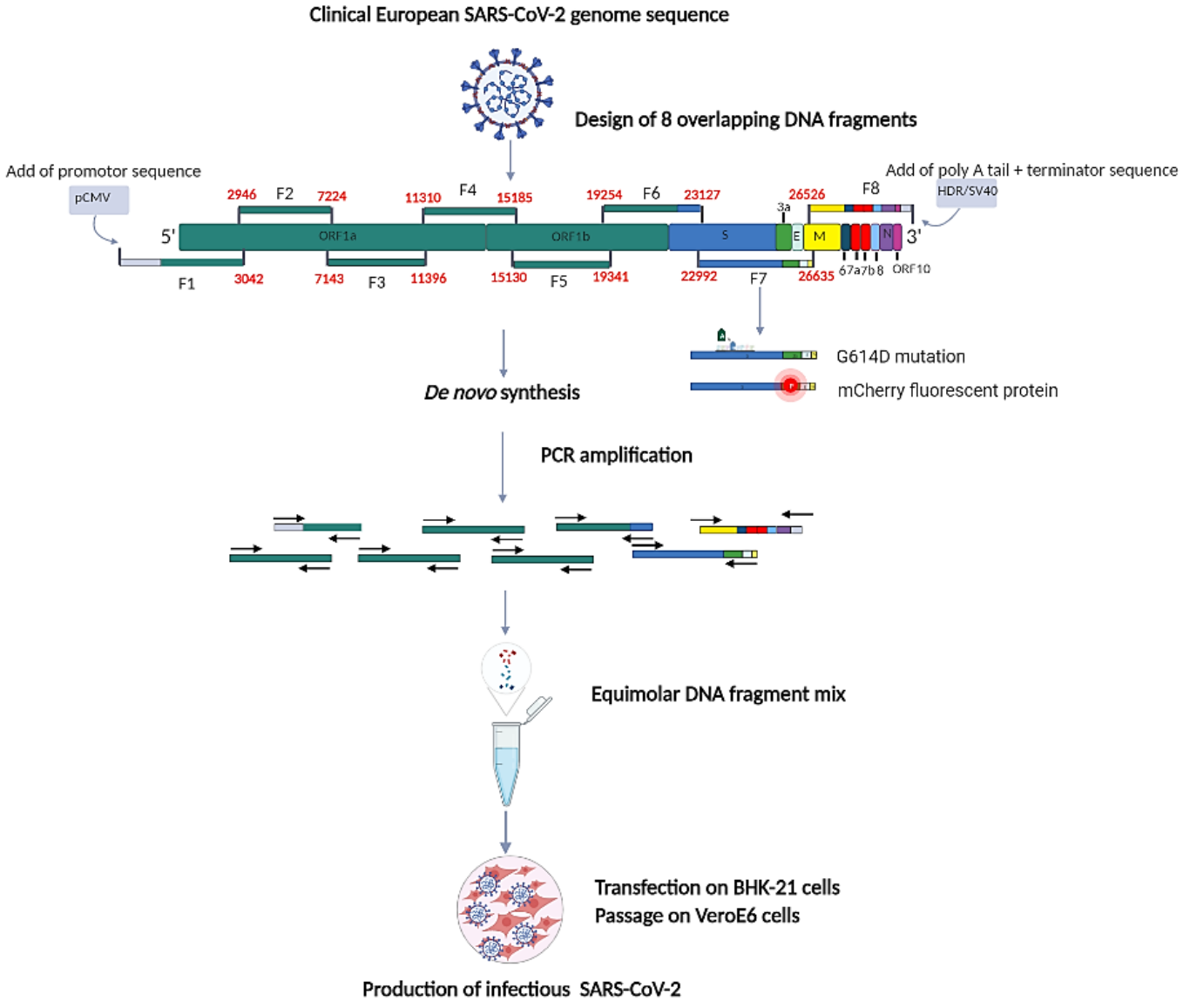

Figure 2. **Virus replication kinetics of clinical and ISA strains.** An MOI of 0.001 and 0.01 were used to infect VeroE6 and FeA cells with rescued or isolated SARS-CoV-2 variants (a) and FeCoV (b) respectively. Data are represented as mean ± SD. Each experiment was performed in triplicate (*N*=3). Exploratory analyses were performed using a two-way ANOVA for multiple comparisons with Sidak's multiple comparisons test.

Statistical comparisons were performed between SARS-CoV-2 clinical European *vs* ISA European strains, ISA European *vs* ISA D614 strains, ISA D614 *vs* mCherry D614 strains and between FeCoV clinical *vs* ISA strains. Only p-values ≤0.05 were indicated. ***, ** and * symbols indicate that the average value for the ISA D614 strain is significantly different from that of the ISA European strain with p-values <0. 0001, <001 and ≤0.05 respectively.

a

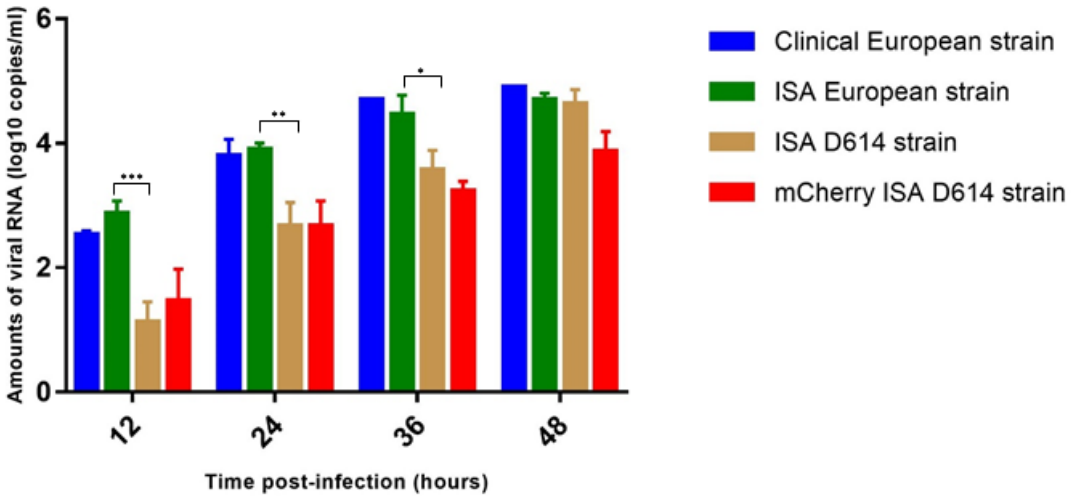
Amounts of viral RNA (log10 copies/ml)
0
2
4
6
***
**
*
12
24
36
48
Time post-infection (hours)
Clinical European strain
ISA European strain
ISA D614 strain
mCherry ISA D614 strain

b

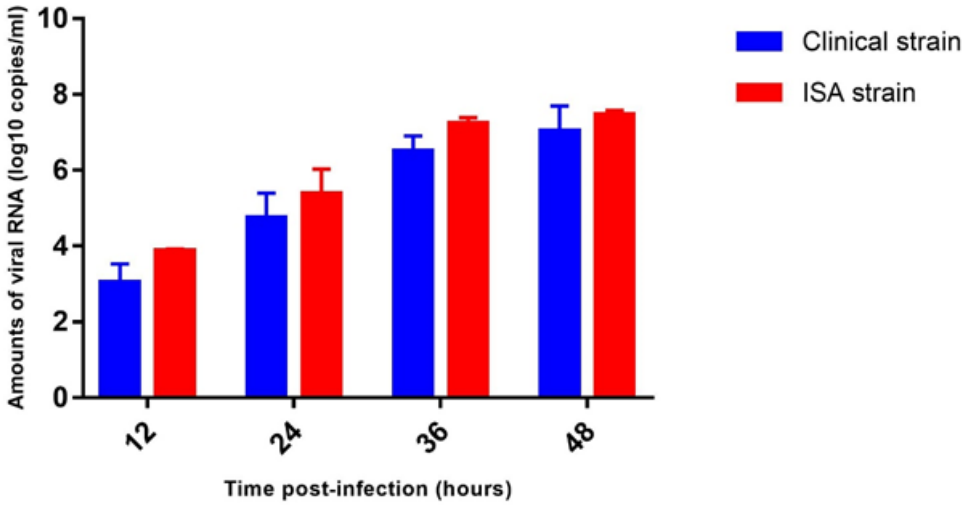
Amounts of viral RNA (log10 copies/ml)
0
2
4
6
8
10
12
24
36
48
Time post-infection (hours)
Clinical strain
ISA strain

579

580

Figure 3. Fluorescence microscopy analysis of ISA D614 and mCherry D614 strains on VeroE6 infected cells. Vero E6 cells were infected with an MOI of 0.5 with the wild-type ISA D614, fluorescent mCherry D614 strains or mock infected. Pictures were taken at 48h pi (20x).

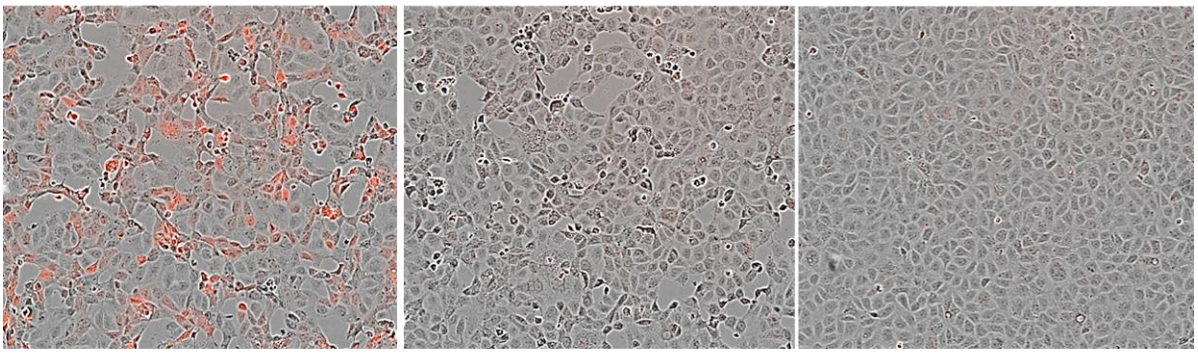

Figure 4. Correlation between neutralizing antibodies (nAbs) titers using ISA D614 and mCherry D614 SARS-CoV-2 strains. A total of 24 human sera were two-fold diluted and incubated with the ISA D614 and mCherry D614 strains and nAb titers were recorded at 5 days post-infection. nAb titers were defined as the highest dilution that inhibited the production of distinct CPE with the ISA D614 SARS-CoV-2 or fluorescence with the fluorescent mCherry D614 SARS-CoV-2. For negative samples, an arbitrary value of 10 was assigned (detection threshold for both methods). Each black dot represents results from a given number of sera. Statistical analysis W performed using univariate linear regression. The error band (in grey) represent the 95% confidence interval of the regression line. The Pearson correlation coefficient (R^2) and *P* value analysis are shown.

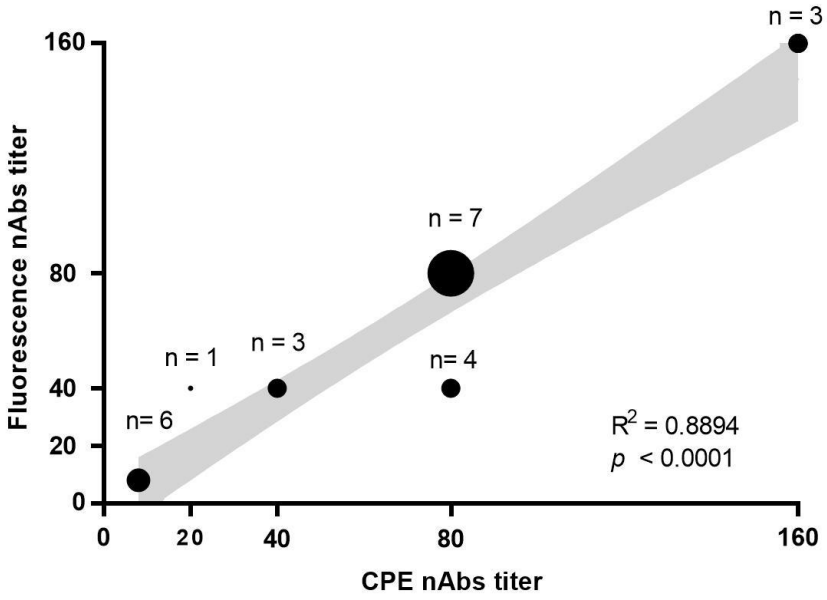

Figure 5. Remdesivir antiviral activity on SARS-CoV-2 in VeroE6 cells.

a: Dose response curve for the ISA D614 and for the mCherry D614 strains obtained by fluorescence or viral RNA measurement in VeroE6 cells; b: Table of EC50 values obtained for the two different strains; c: Fluorescence of the SARS-CoV-2 mCherry in VeroE6 cells with different Remdesivir concentration. EC50: 50% inhibition, Remdesivir concentrations are presented in log scale for logarithmic interpolation. For the ISA D614 strain values are presented from two independent experiments but graphical representation is from one representative experiment. Dose response curves were generated using GraphPad Prism software version 7.0 (https://graphpad-prism.software.informer.com/7.0/).

a

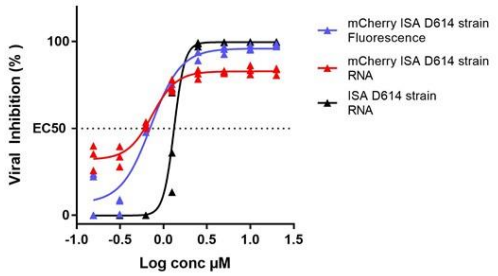

b

	mCherry ISA D614 strain		ISA D614 strain
µM	Viral RNA	Fluorescence	Viral RNA
EC50	0,6	0,7	1,4 ± 0,1

c

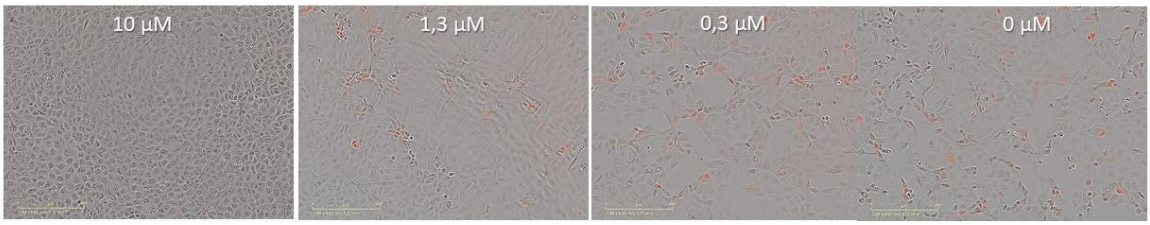

Figure 6. Body weight changes and viral replication in tissues after infection by SARS-CoV-2 in Syrian gold hamsters.

Groups of 4 hamsters were intranasally infected with 10^3 $TCID_{50}$ of clinical European, ISA European or ISA Wuhan strain. a) Clinical course of the disease. Normalized weight at day n was calculated as follows: % of initial weight of the animal at day n. b) Lung infectious titers (measured using a $TCID_{50}$ assay) expressed in $TCID_{50}$/g of lung. c) Lung viral RNA yields (measured using an RT-qPCR assay) expressed in virus genome copy/g of lung. d) Plasma viral loads (measured using an RT-qPCR assay) expressed in viral genome copies/mL of plasma. All graphs represent mean ±SD. ** and * symbols indicate significant difference with a p-value ranging between 0.001-0.01 and 0.01-0.05 respectively (details in supplemental tables 7 and 8).

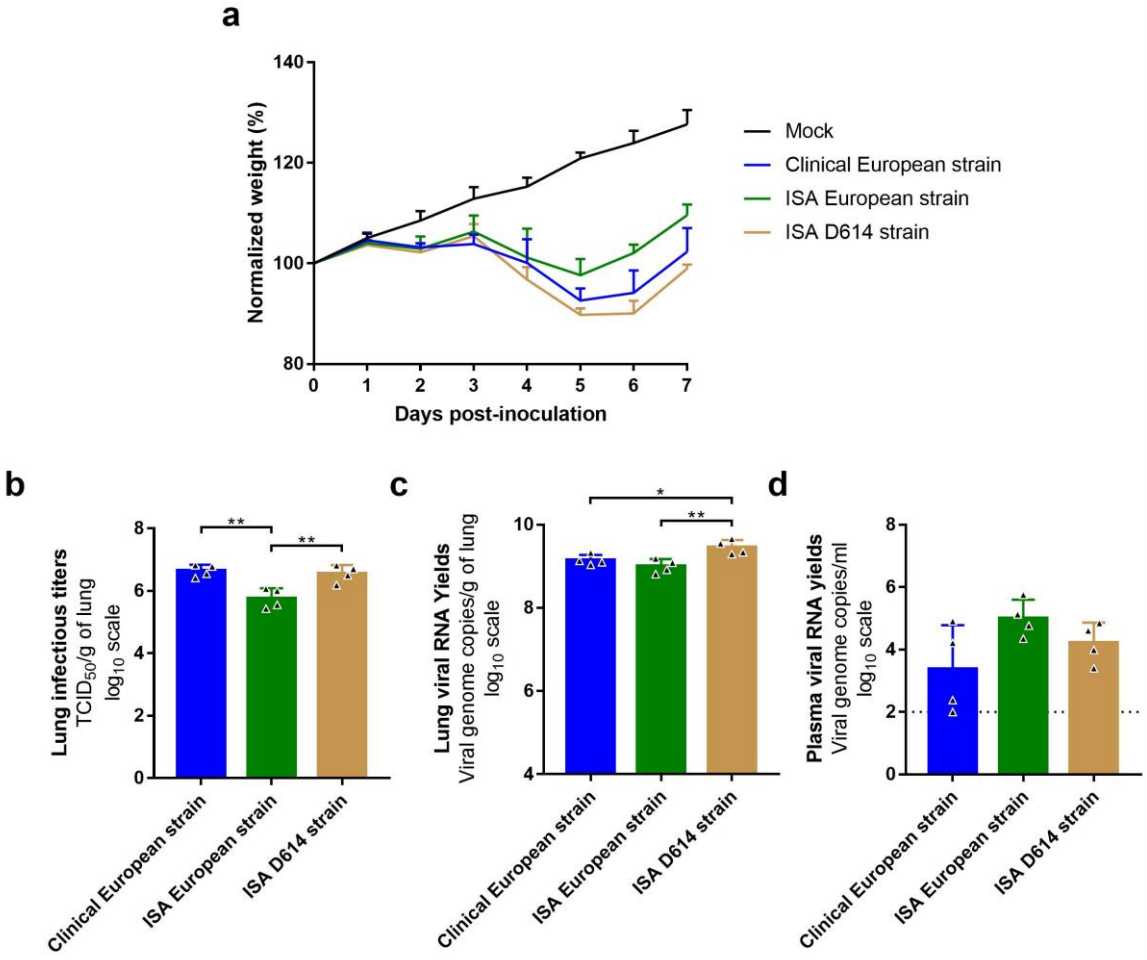

627 **Supplementary Materials**

628 **Supplemental Table 1**. Primers used to amplify cDNA from *de novo* synthesized fragments.

Virus	Fragment	Primer Forward	Primer Reverse	Position
SARS-CoV-2	1	TCAATATTGGCCATTAGCCATA	GGGTAGAAAGAACAATACATATGTG	start-3042
	2	GCATTGATTTAGATGAGTGGAGTATG	GCAGTTAAATCCCATTTAAAAGATG	2946-7224
	3	GTGGTTTAGATTCTTTAGACACC	GTGTCCACACTCTCCTAGCACC	7143-11396
	4	GTGTTATGTATGCATCAGCTG	GTGGCGGCTATTGATTTCAAT	11310-15185
	5	AGTACTATGACCAATAGACAGTTTC	ACTTTTATCAAAAGCTGGTGTGTGG	15130-19341
	6	GCTATCTAACCTTAACTTGCC	GCTGGTGCATGTAGAAGTTC	19254-23127
	7	GCACACCTTGTAATGGTGTTG	GCAAATTGTAGAAGACAAATCC	22992-26635
	8	GCAGATTCCAACGGTACTATTACC	AATTTCACAAATAAAGCATTTTTTTC	26526-end
FeCoV	1	GAATAAGGGCGACACGGAAA	GCATCAGAATCGCTTTTG	start-3291
	2	GGGTGTAGAACTTGAAGGCT	GGGTTGTTGCATGGTAGGAA	3166-6553
	3	GCTGGTTTTTGCATGTTGTC	AAACTAAGAATCATAGCA	6438-10755
	4	GTGTTTACCAATTTACGGTT	GGCTAGCATAAAACTCTTCA	10656-15139
	5	GGGTTAAACATCTACAGAAA	AAATAATAATGGTTTACC	15029-20756
	6	GTATTTTAATAATATAC	ATCTGTTGGTTTTTATTC	20669-23632
	7	GCAGTAGCAGTACAGGCTAG	ATCATTATTCTTCCGACC	23562-27105
	8	AAATGGCCACACAGGGAC	CTCAGGGTCAATGCCAGCGC	27012-end

629

630

Supplemental Table 2. Melting temperature (Tm) of primers during synthetic fragments amplification.

Virus	Fragment	Tm (°C)
SARS-CoV-2	1	55
	2	55
	3	55
	4	61
	5	60
	6	57
	7	60
	8	60
FeCoV	1	60
	2	58
	3	56
	4	58
	5	55
	6	55
	7	58
	8	58

634 **Supplemental Table 3**. Cell lines for which transfections had been attempted to rescue SARS-
635 CoV-2 and FeCoV. Transfections were performed either on one cell line, (condition 1) two cell
636 lines (condition 2) or one cell line with addition of a second cell line 24 hours after transfection
637 (condition 3).

638

639

640

Virus	Condition 1	Condition 2		Condition 3	
	Cell line	Cell line 1	Cell line 2	Cell line 1	Cell line 2
SARS-CoV-2	BHK-21	BHK-21	VeroE6	BHK-21	VeroE6
		BHK-21	BGM		
		BHK-21	A549		
		BHK-21	Huh7		
	HEK-293	HEK-293	VeroE6	HEK-293	VeroE6
		HEK-293	BGM		
		HEK-293	A549		
		HEK-293	Huh7		
	BGM	BGM	A549		
			Huh7		
	A549	A549	Huh7		
	Huh7				
FeCoV	BHK-21	BHK-21	FeA		
		BHK-21	Fcw		
		BHK-21	A-72		
		BHK-21	FeA		
	HEK-293	HEK-293	FeA		
		HEK-293	AK-D		
		HEK-293	Fcw		
		HEK-293	A-72		
		HEK-293	FeA		
	SW-13	SW-13	FeA		
		SW-13	AK-D		
		SW-13	Fcw		
		SW-13	A-72		
		SW-13	FeA		
	FeA				
	Fcw				
	A-72				

641 **Supplemental Table 4**. Primers and probes used for real time RT-qPCR.

642

Length (bp)	Primer Forward	Probe	Primer Rev
61	GGCCGCAAATTGCACAAT	CCCCCAGCGCTTCAGCGTTCT	CCAATGCGCGA
118	GCATGGCTTGCTACGCTCAT	CGCCACCAACGGT	CTCAATCCGGACT
100	CTCTGAGAGCGGCTCTATTGGT	CAGACACGCGGTCCGCTATAACGA	GTTCCCTACAACGA

643

Supplemental Table 5. Neutralizing antibodies (nAb) titers using ISA D614 and mCherry D614 SARS-CoV-2 strains. A total of 24 human sera were two-fold diluted and incubated with the ISA D614 and mCherry D614 strains. nAb titers were recorded at 5 days post-infection. Titers were defined as the highest dilution that inhibited the production of distinct CPE with the ISA D614 SARS-CoV-2 or fluorescence with the fluorescent mCherry D614 SARS-CoV-2.

	nAb titers	
Sera n°	**ISA D614 strain**	**mCherry D614 strain**
1	40	20
2	40	40
3	40	40
4	40	40
5	40	80
6	40	80
7	40	80
8	40	80
9	80	80
10	80	80
11	80	80
12	80	80
13	80	80
14	80	80
15	80	80
16	160	160
17	160	160
18	160	160
19	≤10	≤10
20	≤10	≤10
21	≤10	≤10
22	≤10	≤10
23	≤10	≤10
24	≤10	≤10

Supplemental Figure. The ISA method to rescue FeCoV. FeCoV complete genome sequence was used to design eight overlapping subgenomic viral fragments covering the full genome. Positions on the genome (in nucleotide) are indicated in bold red.